

REPORT DOCUMENTATION PAGE

Form Approved
OMB No. 0704-0188

Public reporting burden for this collection of information is estimated to average 1 hour per response, including the time for reviewing instructions, searching existing data sources, gathering and maintaining the data needed, and completing and reviewing this collection of information. Send comments regarding this burden estimate or any other aspect of this collection of information, including suggestions for reducing this burden to Department of Defense, Washington Headquarters Services, Directorate for Information Operations and Reports (0704-0188), 1215 Jefferson Davis Highway, Suite 1204, Arlington, VA 22202-4302. Respondents should be aware that notwithstanding any other provision of law, no person shall be subject to any penalty for failing to comply with a collection of information if it does not display a currently valid OMB control number. **PLEASE DO NOT RETURN YOUR FORM TO THE ABOVE ADDRESS.**

1. REPORT DATE (DD-MM-YYYY) 30-05-2006		2. REPORT TYPE Technical Paper		3. DATES COVERED (From - To)	
4. TITLE AND SUBTITLE Numerical Simulation of a Thrust Augmented Rocket Nozzle (Preprint)				5a. CONTRACT NUMBER F04611-02-C-0001	
				5b. GRANT NUMBER	
				5c. PROGRAM ELEMENT NUMBER	
6. AUTHOR(S) Roger L. Davis (UC Davis); Melvin J. Bulman & Clement Yam (Aerojet)				5d. PROJECT NUMBER 484702JT	
				5e. TASK NUMBER	
				5f. WORK UNIT NUMBER	
7. PERFORMING ORGANIZATION NAME(S) AND ADDRESS(ES) Aerojet P.O. Box 13222 Sacramento CA 95813-6000				8. PERFORMING ORGANIZATION REPORT NUMBER AFRL-PR-ED-TP-2006-193	
9. SPONSORING / MONITORING AGENCY NAME(S) AND ADDRESS(ES) Air Force Research Laboratory (AFMC) AFRL/PRS 5 Pollux Drive Edwards AFB CA 93524-70448				10. SPONSOR/MONITOR'S ACRONYM(S)	
				11. SPONSOR/MONITOR'S NUMBER(S) AFRL-PR-ED-TP-2006-193	
12. DISTRIBUTION / AVAILABILITY STATEMENT Approved for public release; distribution unlimited (AFRL-ERS-PAS-2006-140)					
13. SUPPLEMENTARY NOTES Presented at the 42 nd AIAA/ASME/SAE/ASEE Joint Propulsion Conference, Sacramento, CA, 9-12 July 2006.					
14. ABSTRACT Numerical results are presented from a reacting-flow Navier-Stokes simulation of a rocket nozzle in which fuel is injected downstream of the nozzle throat for the purposes of augmenting the thrust. The numerical results are compared with experimental data in terms of overall thrust and specific impulse as well as pressure distribution along the nozzle wall. The flow physics associated with the thrust augmentation is also described. The investigation shows that propellant injection downstream of the throat is a viable method for augmenting rocket thrust. In addition, the augmented thrust levels increase with increasing levels of injected mass flow. Finally, the investigation shows that the numerical predictions are in good agreement with the experimental results.					
15. SUBJECT TERMS					
16. SECURITY CLASSIFICATION OF:			17. LIMITATION OF ABSTRACT	18. NUMBER OF PAGES	19a. NAME OF RESPONSIBLE PERSON
a. REPORT	b. ABSTRACT	c. THIS PAGE			Stephen Hanna
Unclassified	Unclassified	Unclassified	A	11	19b. TELEPHONE NUMBER <i>(include area code)</i> N/A

Numerical Simulation of a Thrust Augmented Rocket Nozzle (Preprint)

Roger L. Davis*

University of California at Davis, Davis, California, 95835

Melvin J. Bulman[†] and Clement Yam[‡]

GenCorp Aerojet, Rancho Cordova, California, 95670

Numerical results are presented from a reacting-flow Navier-Stokes simulation of a rocket nozzle in which fuel is injected downstream of the nozzle throat for the purposes of augmenting the thrust. The numerical results are compared with experimental data in terms of overall thrust and specific impulse as well as pressure distribution along the nozzle wall. The flow physics associated with the thrust augmentation is also described. The investigation shows that propellant injection downstream of the throat is a viable method for augmenting rocket thrust. In addition, the augmented thrust levels increase with increasing levels of injected mass flow. Finally, the investigation shows that the numerical predictions are in good agreement with the experimental results.

Nomenclature

P	=	pressure
M	=	Mach number
TAN	=	thrust augmented nozzle
X	=	axial distance along nozzle
L	=	nozzle length
subscripts		
ref	=	reference conditions
T	=	stagnation conditions

I. Introduction

THURST augmentation in the form of an afterburner has often been used in gas-turbine engines to greatly increase thrust. Jet engine afterburners increase core thrust through the addition of fuel downstream of the low-pressure turbine and combustion that increases the temperature of the exhaust. Although the engine exhaust pressure does not increase, the dramatic increase in the speed of sound leads to a significant increase in the achievable exit velocity, and thus thrust, of the engine. The augmentation in a turbojet engine is limited, however, by the available oxygen unburned in the main combustor. Afterburning can also be used in rocket engines through the combustion of propellants injected downstream of the rocket nozzle throat.

Aerojet has patented an Afterburning Rocket called the Thrust Augmented Nozzle¹ (TAN). Figure 1 shows the TAN concept. Fuel and oxidizer are injected just downstream of the nozzle throat where they burn to increase engine thrust when it is needed most during the first minute after take off from sea level. TAN thrust augmentation is virtually unlimited since both fuel and oxidizer are injected. The TAN concept has been designed and tested at GenCorp Aerojet. Figure 2 shows test firings with TAN on and off. In addition to demonstrating the concepts and advantages of the TAN, the experimental data is also very important in validating computational fluid dynamics

* Professor, Mechanical and Aeronautical Engineering Department, Aerojet Consultant, AIAA Associate Fellow.

[†] Technical Principal, Advanced Development Engineering, Dept. 5276, P.O. Box 13222, Bldg 20019, AIAA Associate Fellow.

[‡] Engineering Specialist, Computational Fluid Dynamics Group, Dept. 5272, P.O. Box 13222, Bldg. 20019.

Distribution A: Approved for public release; distribution unlimited

codes used for design. The present investigation represents a validation of a reacting-flow Navier-Stokes procedure as well as a numerical investigation of the detailed flow physics associated with thrust-augmented nozzles. The detailed information generated from the numerical simulations is impossible to achieve with an experiment due to the severe environment and excessive resources that would be required. Thus, the combination of experimental data and numerical simulation results can provide a much more complete description into the flow physics that occur in this new augmentation device.

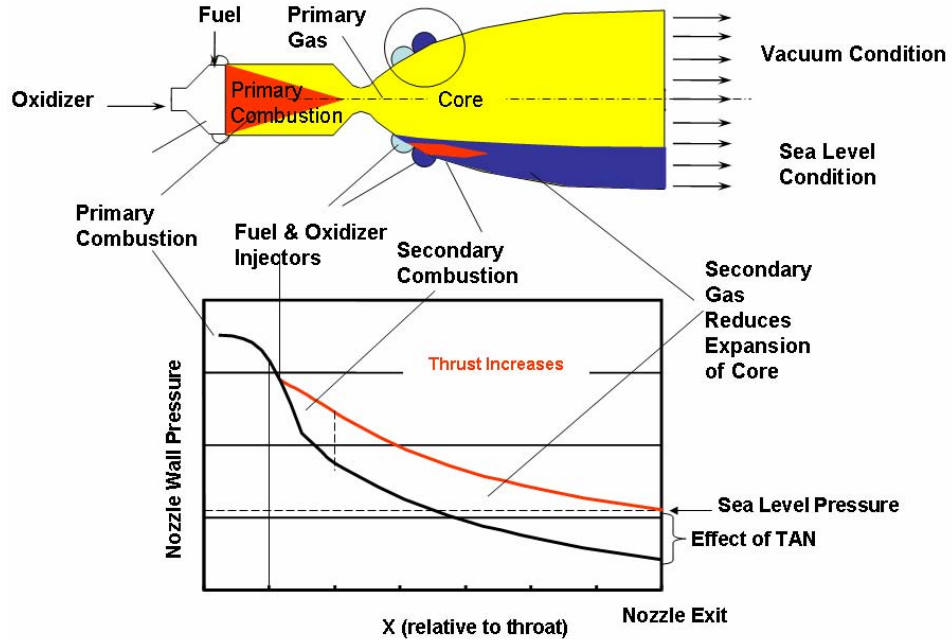


Figure 1. TAN Schematic and Flow Physics

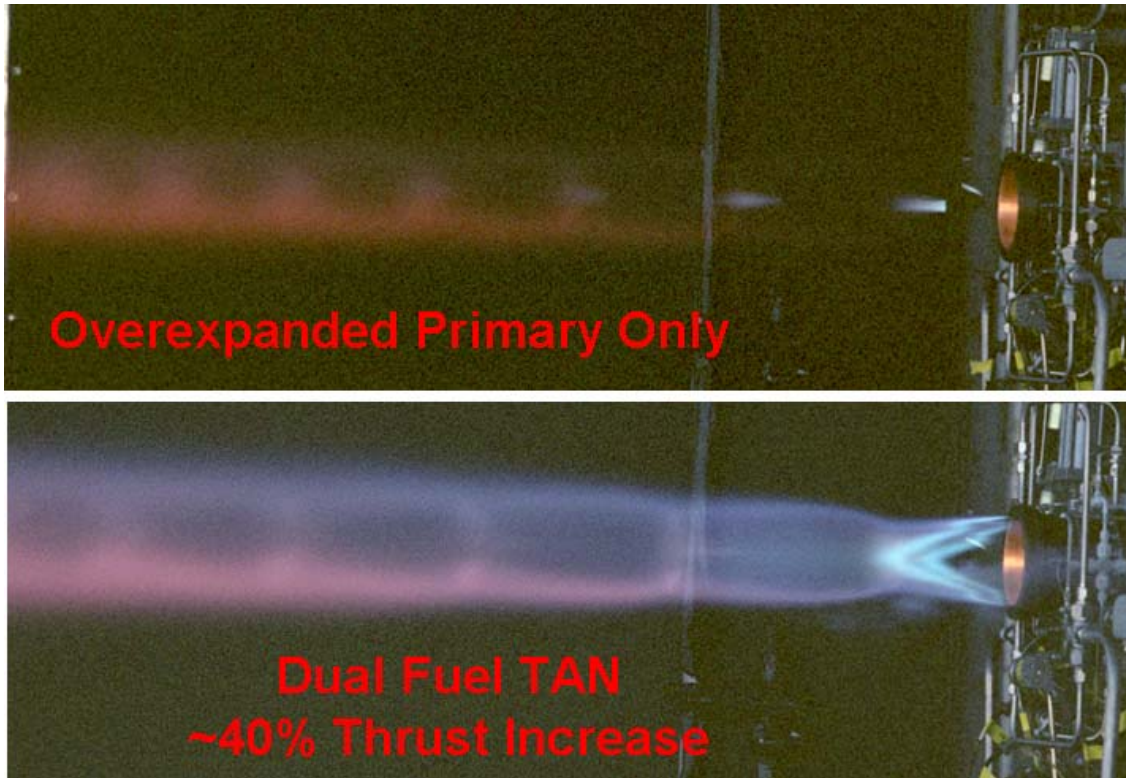


Figure 2. TAN Test Firing at Aerojet

Figure 1 also shows a schematic of the characteristic flow physics of a TAN. Propellants (fuel and oxidizer) are injected downstream of the nozzle throat and act to increase mass and energy exiting the nozzle. For an overexpanded nozzle operating at sea level conditions, the additional mass also acts to reduce the effective nozzle area ratio of the core flow. This reduced effective area correspondingly reduces the core flow average Mach number and raises the nozzle exit pressure such that the thrust penalties associated with overexpansion are greatly reduced. Thus thrust augmentation comes about through added mass, inertia, energy from the TAN propellants as well as from the reduction in overexpansion penalties.

II. Configuration

The liquid rocket engine nozzle shown schematically in Figure 3 was used in the current investigation. High-pressure gaseous hydrogen and oxygen were used as the propellants in the chamber. Rocket propulsion fuel (RP1) and liquid oxygen were injected downstream of the throat at the nozzle wall using injectors that were uniformly spaced circumferentially. Measurements of thrust, chamber injector mass flow rates, and augments mass flow rates were obtained in the experimental program. In addition, the pressure at 10 locations along the nozzle wall was measured to determine the effect of the TAN injection on the wall loading.

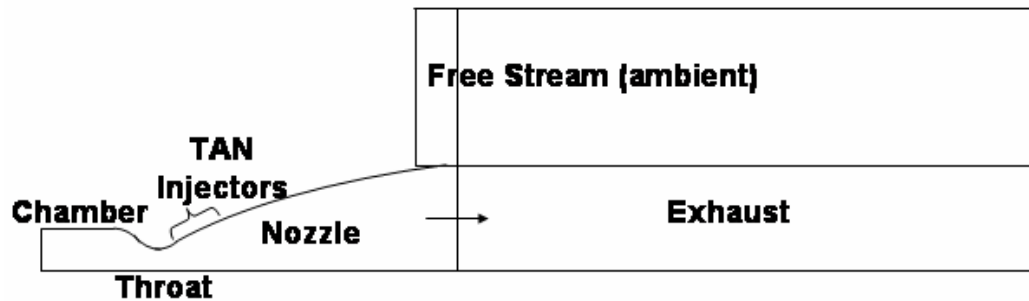


Figure 3. Schematic of Liquid Rocket Engine Configuration with TAN

III. Numerical Simulations

As part of the current investigation, axisymmetric and three-dimensional numerical simulations were performed using the commercially available Fluent code². The current investigation focused on validating the effects of changing augments mass flow and mixture ratio on the thrust and specific impulse.

A. Computational Grids

In these validations, the computational grids were tightly clustered near the chamber/nozzle walls in order to capture the wall-normal gradients in density and velocity. Wall functions were not used in these simulations but rather, the viscous flow was solved directly to the wall. The turbulence model used in Fluent was the RNG $k-\epsilon$ model³, which included wall thermal and pressure gradient effects. The computational grids in these validations were extended beyond and outside of the nozzle exit, as shown in Figure 4. Thus, the nozzle exit flow including the entrained air outside of the nozzle was predicted. The axisymmetric multi-block structured-like grid, consisting of a total of 54,816 nodes, was generated using the Gambit grid generation code².

A three-dimensional computational grid, representing a single TAN injector element was also generated with Gambit. The axisymmetric computational domain shown in Figure 4 was swept circumferentially around the nozzle centerline to create the domain of the three-dimensional model, shown in Figure 5. The injector elements were placed along the wall downstream of the nozzle throat mid-way between the two circumferential boundaries in the three-dimensional simulation. The three-dimensional computational grid, also shown in Figure 5, was created in a similar topology as the axisymmetric grid. The resulting three-dimensional grid contained 1.62 million grid points.

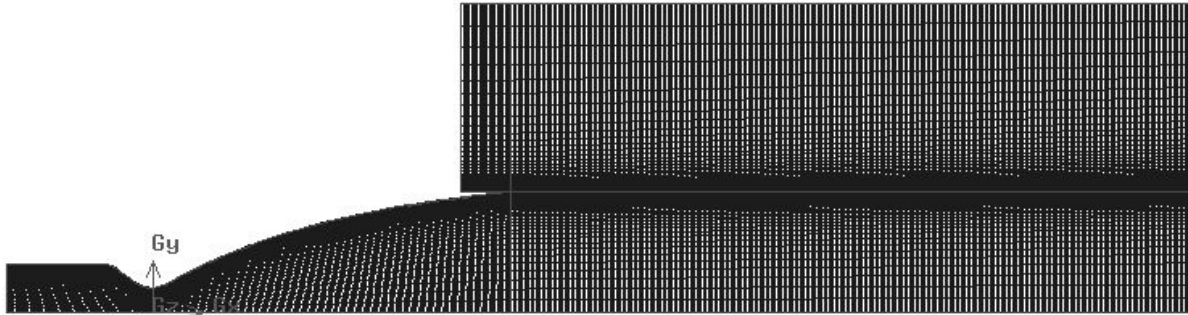


Figure 4. Axisymmetric Computational Grid

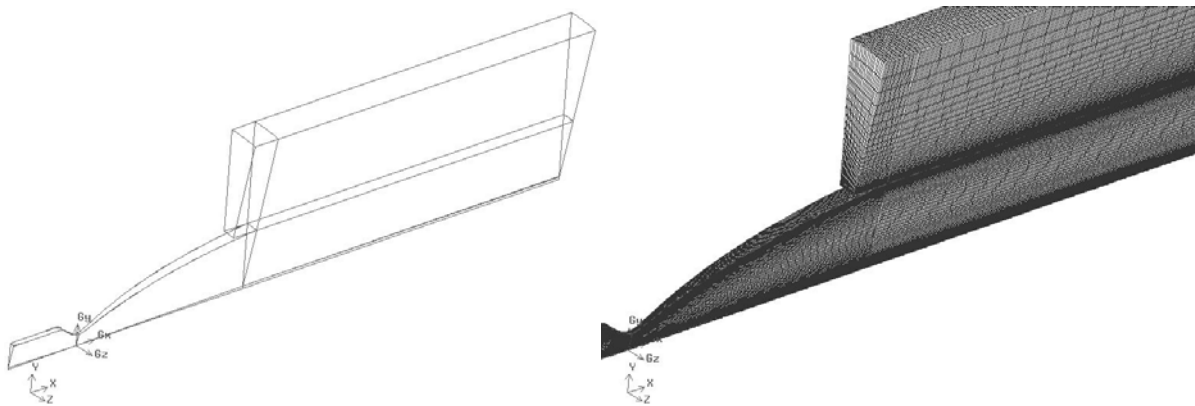


Figure 5. Three-Dimensional Topology and Computational Grid

B. Computational Boundary Conditions

At the upstream boundary (main injector face) of the computational domain, the incoming main injector flow was modeled as products of gaseous hydrogen and oxygen with molecular weight of 5.91 kg/mol (13.031 lbm/mol), molecular viscosity of 9.739×10^{-5} kg/m-s (6.544×10^{-5} lbm/ft-s), and approximated variable specific heat and thermal conductivity, determined from NIST/REFPROP program⁴. The mass flow rate of the main injector was held fixed along with the inlet total pressure and temperature. A thin layer of pure gaseous hydrogen, used as film-cooling in the real configuration, was also injected with a fixed mass flow rate and temperature at the inlet adjacent to the chamber outer wall. The wall of the nozzle and chamber was maintained with a no-slip boundary condition with a fixed wall temperature. The outflow boundaries outside of the nozzle were set to constant sea-level atmospheric pressure. The TAN injector locations were defined at the actual locations of the experiment. The mass flow rate for each TAN fuel and liquid oxygen (LOX) injector was specified by equally distributing the total mass flow rates of the test over the fuel or LOX injectors. The temperature of the injected fuel and LOX was held constant. The droplets of fuel/LOX were injected with specified velocity components and droplet size.

C. Baseline (No Augmentation) Flow Results

The baseline validation corresponded to the experimental conditions with no TAN injection. This simulation provided a comparison between computed and measured thrust and specific impulse with no TAN effects. All simulations were run at least 100,000 iterations in order to arrive at a “steady” solution. The maximum CFL stability condition that could be run in the current axisymmetric simulations was 1.0. The maximum CFL used in the three-dimensional simulations was 0.4.

Figure 6 shows contours of the computed Mach number. To facilitate comparison between the axisymmetric and three-dimensional results, the axisymmetric contours are shown on the bottom half of Figures 6 through 11 whereas the three-dimensional results are shown on the upper half of each figure. The three-dimensional contours in these figures were shown along the $\theta=0^\circ$ circumferential plane (mid-way between two TAN injectors). The thrust and specific impulse of this unaugmented case were used to non-dimensionalize the results shown below to document the effect of augmented mass flow levels on the rocket nozzle performance. Figure 6 shows that the axisymmetric and three-dimensional Mach contours are in very good agreement. The angle of the oblique shock attached to the

nozzle wall at the exit for the three-dimensional simulation is slightly less than that predicted by the axisymmetric simulation. The shape and radius of the plume downstream of the nozzle exit between the two simulations are essentially the same.

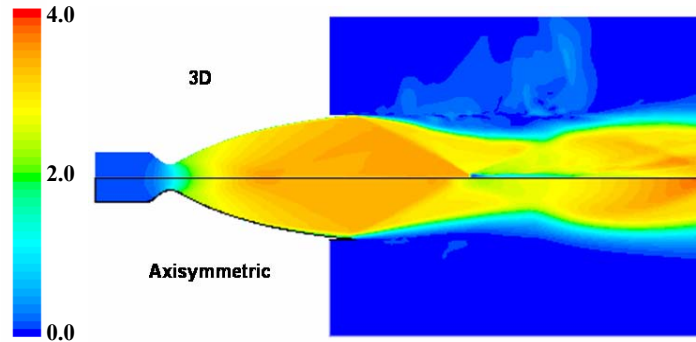


Figure 6. Computed Mach number Contours for Unaugmented Nozzle

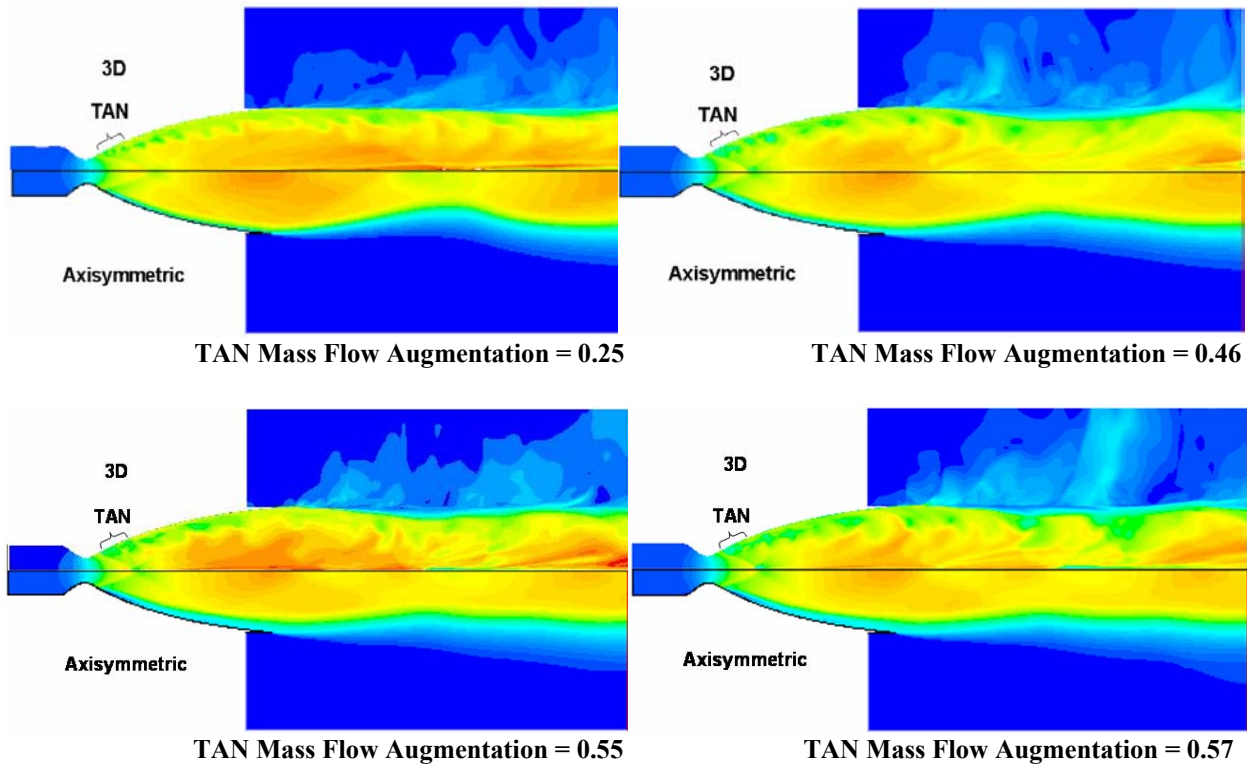


Figure 7. Computed Mach number Contours for Nozzle with Augmentation

D. Effect of TAN Mass Flow on Performance

Contours of the computed Mach number in the computational domain at four different TAN mass flow augmentation values are shown in Figure 7. The contour levels of Figure 7 are the same as those shown in Figure 6. TAN mass flow augmentation is defined as the mass flow rate of injected TAN propellants divided by the total mass flow rate of the chamber. The Mach number contours show that injection of fuel downstream of the throat has the effect of reducing the flow Mach number near the nozzle walls. The three-dimensional simulations exhibit wave-like Mach number contours near the nozzle walls indicating the flow is likely to be unsteady. This is due to the fuel and LOX jet interaction with the gaseous flow to both sides of the injectors circumferentially. This circumferential

interaction is absent in the axisymmetric simulations since the injectors are modeled as slots. The injected fuel and oxidizer effectively change the nozzle shape and area ratio due to the added mass from the TAN injectors. As the injection mass flow increases, the exhaust plume outer radius and Mach number distribution become more uniform in the axisymmetric simulations. The three-dimensional simulations show higher oblique shock wave content in the exhaust plume Mach number contours. An oblique shock is shown near the TAN injection location just downstream of the throat that increases in strength as the injection flow increases.

Figures 8 and 9 show a comparison between the axisymmetric and three-dimensional computed contours of the combustion chamber combusted gas species concentration contours. These contours, along with the Mach number contours shown above can be used to help illustrate the nozzle flow physics associated with injection of propellants downstream of the throat. Figure 8 shows that with no injection, the computed axisymmetric and three-dimensional contours of species concentrations are essentially the same. The shape of the exhaust plume is also essentially the same as expected since there were no geometric or flow conditions that could alter the three-dimensional results from an axisymmetric flow. For the augmented cases, however, the injection of propellants in discrete wall jets downstream of the throat creates significant three-dimensional flow along the wall of the nozzle.

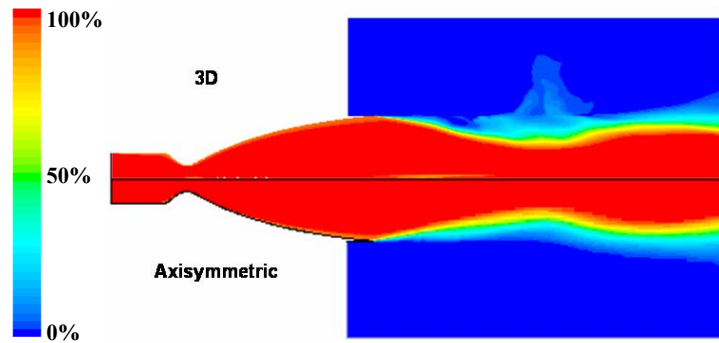


Figure 8. Computed Chamber Combustion Product Contours for Unaugmented Nozzle

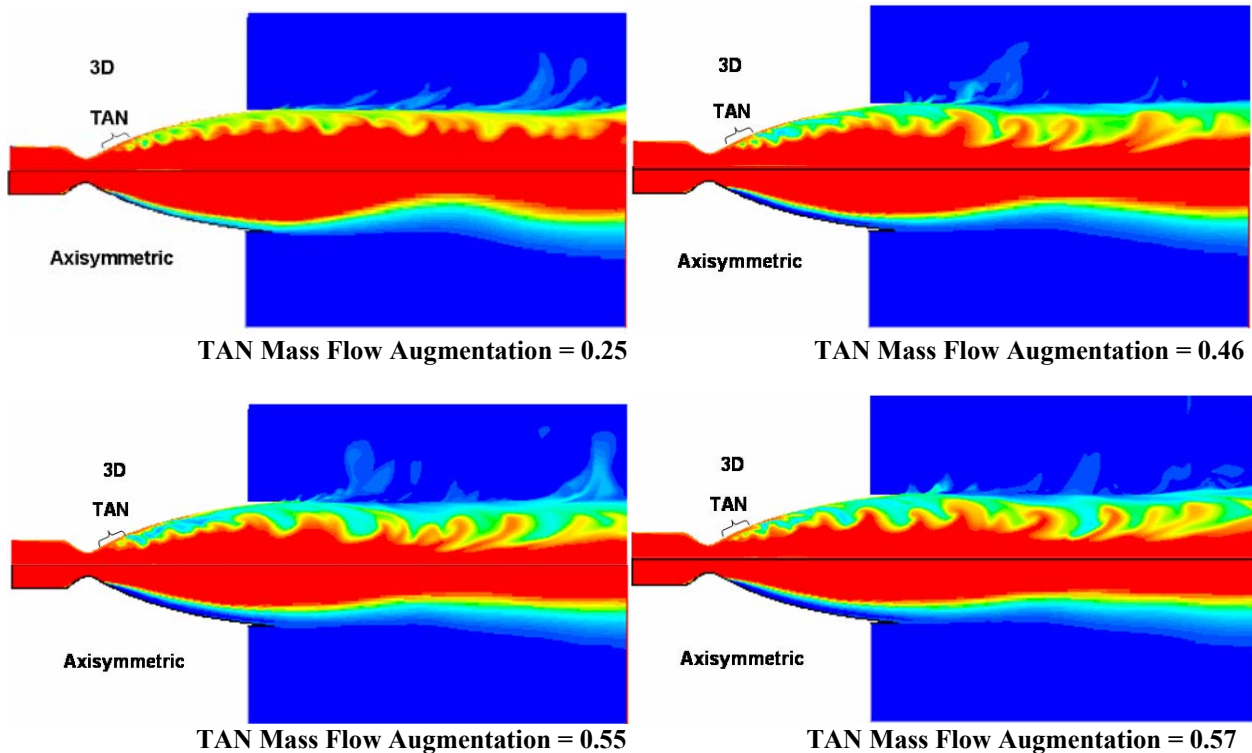


Figure 9. Computed Chamber Combustion Product Contours with Augmentation

Figure 9 shows the comparison of the percent combusted gas species concentrations between the axisymmetric and three-dimensional simulations at the same TAN mass flow augmentation values as shown in Figure 7. As the TAN mass flow increases, the effective diameter of pure combustion chamber products reduces in size downstream of the TAN injection. This behavior is observed in both the axisymmetric and three-dimensional simulations but is more pronounced in the three-dimensional results due to the much stronger mixing. As a result, the chamber gases expand through an effective nozzle area ratio that is reduced from the actual physical geometry thereby reducing the average Mach number in the core and increasing the average pressure at the exit of the nozzle. For the unaugmented rocket nozzle expanding into sea level atmosphere, the exit flow from the nozzle is overexpanded. Thus, the unaugmented nozzle core exit pressure is nominally much lower than atmospheric pressure. As a result, thrust is lost proportional to the nozzle exit area times the difference in pressure between the nozzle exit flow and atmosphere. However with augmentation, the average nozzle exit pressure increases with increases in TAN mass flow, thereby lowering the thrust penalty due to the overexpanded nozzle. In addition, as described below, TAN injection improves thrust further from the added fluid inertia and energy release.

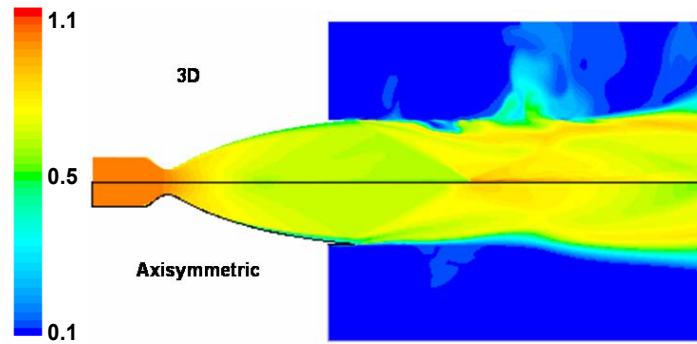


Figure 10. Computed Non-Dimensional Temperature Contours for Unaugmented Nozzle

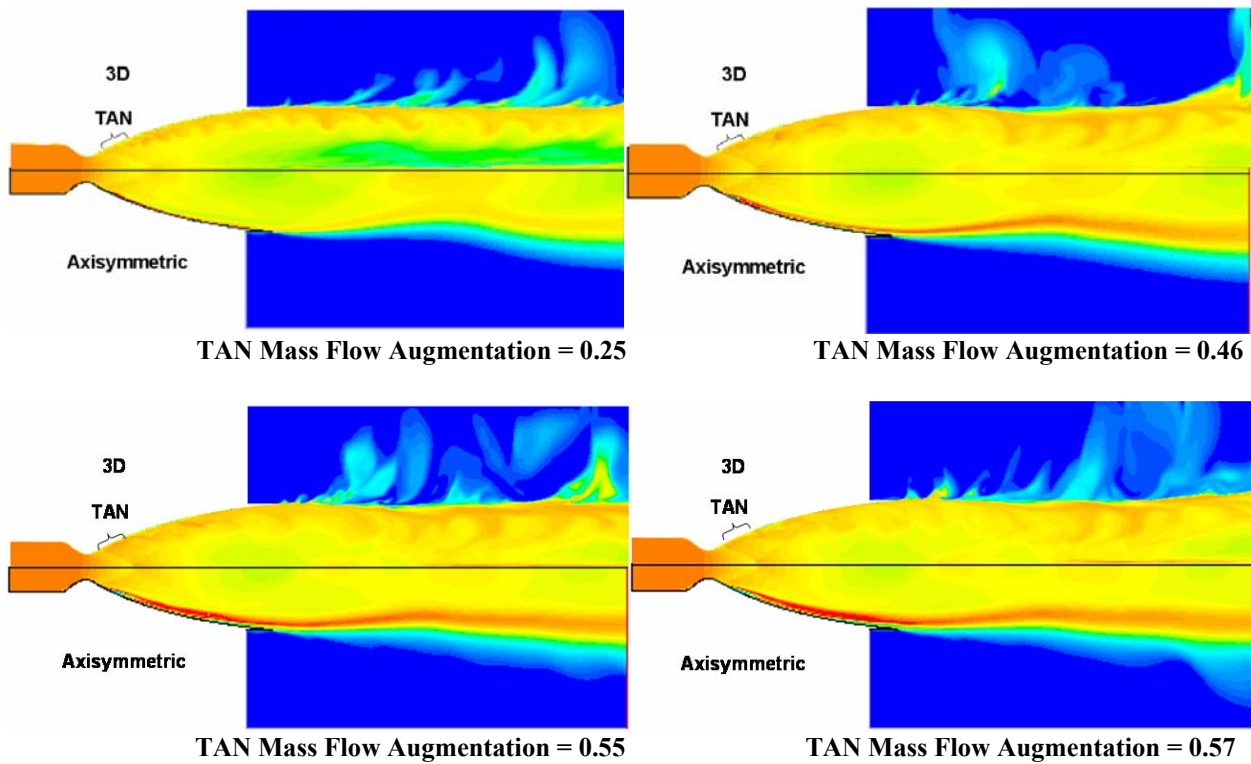


Figure 11. Computed Non-Dimensional Temperature Contours with Augmentation

The computed temperature contours resulting from the axisymmetric and three-dimensional simulations are shown in Figure 10 for the nozzle without TAN injection and in Figure 11 for the various TAN mass flow levels. The temperature is non-dimensionalized by the chamber temperature in these figures. These figures show that the temperature in the gas adjacent to the nozzle wall increases with the amount of injected propellants. Comparison between the axisymmetric and three-dimensional results show that the higher temperature gas associated with the reacting TAN injection flow is greater in the axisymmetric simulations than in the three-dimensional simulations. Figure 11 also shows that the thickness of the flow region associated with the TAN injected propellants adjacent to the nozzle wall is thinner for the axisymmetric simulation than for the three-dimensional result. The higher mixing in the three-dimensional simulation distributes the high gas temperature adjacent to the nozzle wall and increases the thickness of the layer of reacting gas adjacent to the wall. The TAN propellants burn with a lower total temperature than the core propellants but are moving at a lower Mach number. The higher temperature in the TAN reacting gas flow corresponds to the higher energy content of that part of the flow. So even though the average core Mach number and momentum at any axial station decreases due to the reduced effective area, this loss is offset by reduction in the thrust penalty from the overexpansion at the nozzle exit. The increased core thrust and additional momentum from the combusted TAN propellants, are responsible for total increases in thrust (augmentation) observed.

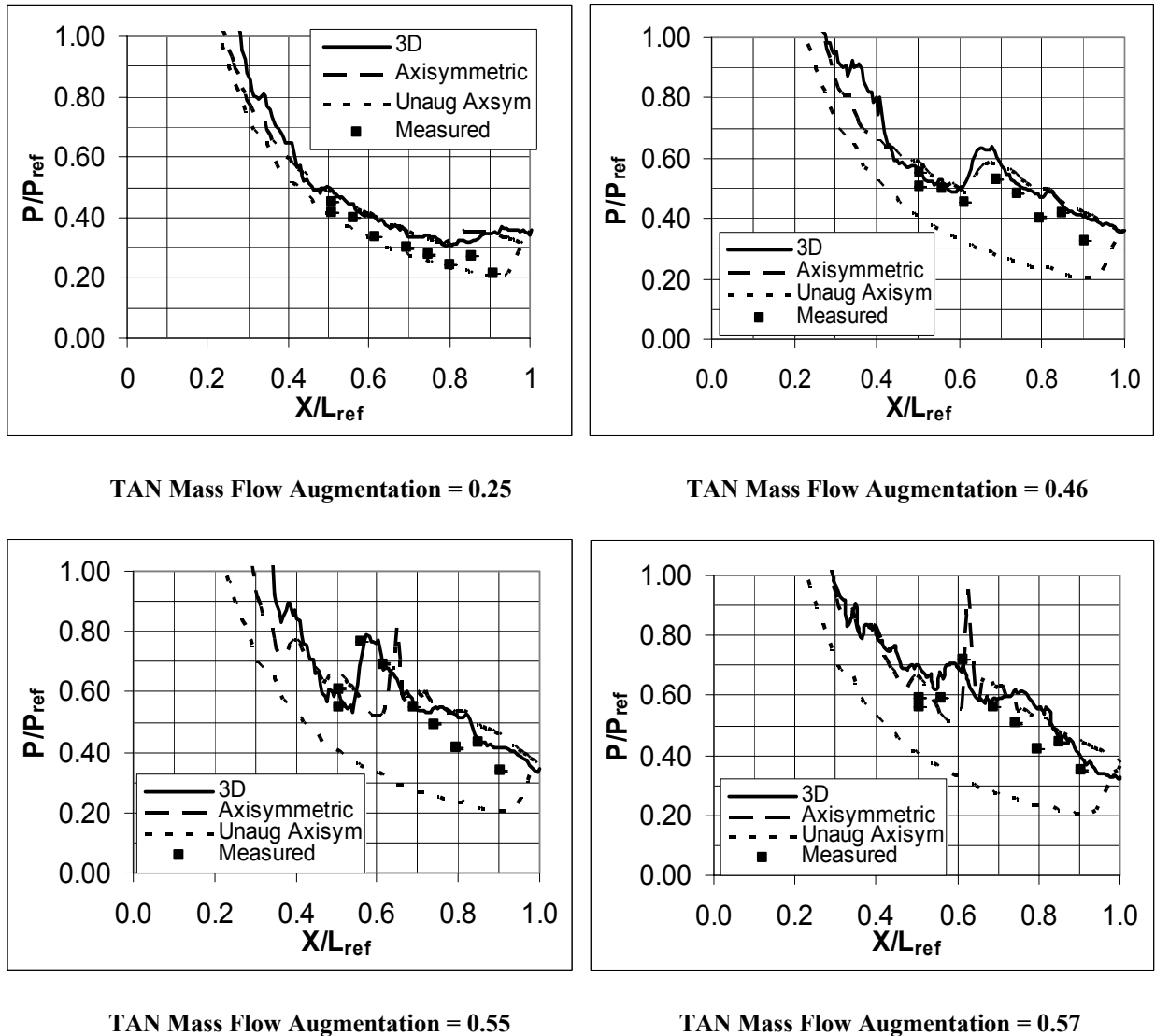


Figure 12. Comparison between Computed and Measured Nozzle Wall Pressure

A comparison between the predicted and measured nozzle wall pressure at the four different injector mass flow levels is shown in Figure 12. The unaugmented computed pressure distribution from the axisymmetric simulation is shown in the various pressure distribution plots as a baseline for comparison with the augmented pressure distributions. Comparison between the predicted nozzle wall pressure and the measured pressure is good. The computed pressure from the three-dimensional simulations, in general, agrees with the experimental data better than those from the axisymmetric simulations. As discussed above, the levels of both computed and measured pressure increase with increasing TAN mass flow as can be seen by comparison with the unaugmented axisymmetric computed pressure distribution. The increase of pressure levels further substantiate that the Mach numbers exiting the nozzle decrease somewhat due to the reduction in the effective nozzle area ratio as the TAN flow increases.

The jump in pressure resulting from the oblique shock generated by the augmentation injection can be seen in both the prediction and measurements of Figure 12 at a non-dimensional axial location between 0.55 and 0.7 depending on the injected propellant mass flow levels. The computed shock location is in good agreement with the measured location except for the TAN mass flow augmentation level of 0.55 where the measured data indicates that the oblique shock strikes the nozzle wall upstream of where it is computed to be by the axisymmetric simulation. The computed oblique shock strength is in good agreement with the measured value except at the TAN mass flow augmentation level of 0.57 where the axisymmetric computed strength is greater.

A comparison between the computed and measured thrust augmentation of the nozzle as a function of TAN mass flow augmentation is shown in Figure 13. Thrust augmentation is defined as the percent increase in thrust as compared to the unaugmented thrust. Figure 13 shows that the overall thrust of the nozzle increases significantly from the TAN injection. The additional mass, inertia, and energy produced from the TAN reaction as well as the reduction in thrust penalty due to overexpansion significantly increases thrust compared to the unaugmented nozzle. The axisymmetric and three-dimensional simulation computed values of thrust augmentation are overall, in reasonably good agreement with the measured values. The axisymmetric computed results are slightly high for the thrust augmentation whereas the three-dimensional computed results are slightly lower. The difference between the axisymmetric computed and measured thrust augmentation is a maximum of 3% with the average difference being 1.5%. The maximum difference between the three-dimensional computed and measured thrust augmentation is a maximum of 8.5% with the average difference being 2.4%.

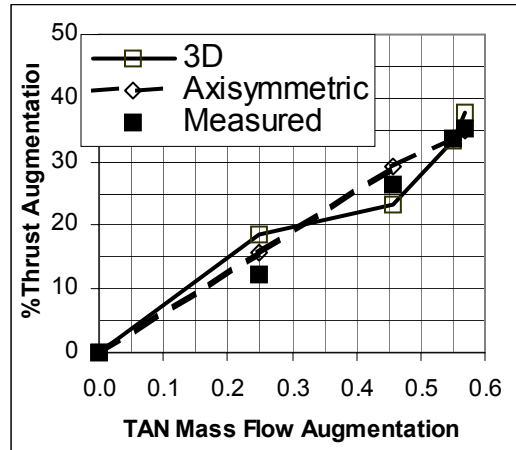


Figure 13. Comparison between Computed and Measured Thrust Augmentation

IV. Conclusions

The commercially available Fluent reacting-flow Navier-Stokes code has been validated against experimental data for reacting flow in a thrust augmented liquid rocket nozzle. Both axisymmetric and three-dimensional simulations have been performed and the results have been compared with experimental data. Comparisons show that the axisymmetric and three-dimensional computations are on average within 3% of predicting the absolute levels of thrust and specific impulse and predict the trends in performance as a function of the TAN augmentation mass flow well. The simulations and data show that the thrust can be augmented significantly through the use of augmentation. Testing has shown that even greater thrust augmentation can be achieved through greater TAN mass flow augmentation than investigated here. The numerical simulations show that the increase in thrust arises from

the increase in mass flow, inertia, and energy exiting the nozzle resulting from the TAN injection propellants as well as a reduction in thrust penalties from overexpansion brought about by the reduction in effective core nozzle area.

Acknowledgments

The authors would like to thank the managers at GenCorp Aerojet and the US Government for their support and permission to publish this material.

References

¹U. S. Patent 6,568,171

²FLUENT, Version 6.2.16 User's Manual

³Yakhot, V. and Orszag, S. A., "Renormalization Group Analysis of Turbulence", Journal of Scientific Computing, Vol 1, No. 1, March 1986.

⁴National Institute of Standards and Technology (NIST), E.W. Lemmon, A. P. Peskin, M.O. McLinden, and D. G. Friend, National Institute of Standards and Technology, Boulder, CO